Fusion of Histological Sections and MR Images: Towards the Construction of an Atlas of the Human Basal Ganglia

S. Ourselin[1], E. Bardinet[1], D. Dormont[3], G. Malandain[1], A. Roche[1], N. Ayache[1], D. Tandé[2], K. Parain[2], and J. Yelnik[2]

[1] INRIA, Epidaure Project, Sophia Antipolis, France
[2] INSERM U289, Salpêtrière Hospital, France
[3] Neuroradiology Dept and LENA UPR 640-CNRS, Salpêtrière Hospital, France

Abstract. In neurosurgery, localisation of deep brain structures is a crucial issue, which can be assisted by a 3-dimensional brain atlases. Our goal is to build such an atlas by fusing histological data with a 3D MR image of the same subject. This requires two steps: first a 2D realignment of the histological sections in order to obtain a three-dimensional block, then a 3D registration between this reconstructed block and the MR image. Both steps are based on the same robust registration algorithm.

1 Introduction

Accurate localisation of brain structures is a crucial issue for neuro-scientists. Recently, a new surgical treatment of Parkinson's disease consisting of deep brain stimulation (DBS) has been developed. In the first attempts, the target was in the thalamus [2], then moved to the internal globus pallidus, and finally to the sub-thalamic nucleus [5]. In this procedure, the surgical success depends primarily on the localisation of the target. Up to now, the target has been localised using ventriculographic landmarks [1] or MR images [3] in stereotactic conditions, and a statistical estimation based on an anatomical atlas, usually the Schaltenbrand and Wahren [13] or Talairach and Tournoux atlases [15].

However, for such a purpose, information provided by such atlases present several drawbacks: 3-dimensional alignment of contiguous sections has not been verified; the atlas resolution (from 1 to 4 mm in Z direction) is not sufficient for a precise localisation (e.g. the sub-thalamic nucleus is viewed in very few slices of the Schaltenbrand atlas); cerebral contours are not in a form suitable for automatic registration with digital MR images of individual patients.

Using interpolation, it is possible to generate an isotropic (with a constant inter-slice distance of 0.5 mm) Schaltenbrand atlas [18]. This improves the consistency of the atlas for visualisation and manipulation purposes, but not from an anatomical point of view as the necessary information is still missing. Moreover, interpolation is sensitive to wrong alignment between the original sections.

Therefore, to determine with accuracy the DBS target localisation, the key issue appears to be the construction of a 3D atlas of the human basal ganglia,

W. Niessen and M. Viergever (Eds.): MICCAI 2001, LNCS 2208, pp. 743–751, 2001.

designed for further propagation onto the MR acquisition of a given patient, to allow a precise surgery planning.

We present here the first steps of the construction of an atlas of the human basal ganglia designed for our purpose, built by fusing a *post mortem* MR T1-weighted 3D image with a series of 2D histological sections. Superimposition onto the MR acquisition of a given patient could then be achieved by elastic matching (e.g. [**?**]). Data acquisition is detailed in section 2. Fusion methods and results are given in section 3.

2 Data Acquisition and Preprocessing

2.1 MR Images

The MR study was conducted 36 hours after death, before extraction of the brain. It consisted of a T1-weighted acquisition in the axial plane ($256 \times 256 \times 124$, $0.9375 \times 0.9375 \times 1.3$ mm^3). A T2-weighted image in the coronal plane is acquired too, but was not used in this study.

2.2 Histological Sections

After MR acquisition, the brain was processed for histology.

- The brain was stored in 4% paraformaldehyde for 8 days and in phosphate buffer with sucrose for 7 days. In this process, the brain, and especially the ventricles, were submitted to a global compression.
- One hemisphere was sectioned into 4 blocks (1.5 cm thick) in order to favour a better fixation, and stored frozen at -40^oC, which causes a global shrinkage.
- The blocks were cut into 70 μm thick sections which were collected serially. Sectioning was done on a Tetrander Jung freezing microtome.

During the two first steps of the procedure, global distortions of the histological block with respect to the *ground truth* occur, and the ventricles almost collapse, while the third step caused slight uncorrelated local non-linear distortions on each section.

Sections were treated according to different immunohistochemical procedures. One out of ten sections (thus every 700 μm) was stained using the Nissl technique (Figure 1) to reveal cytoarchitectonic contours of cerebral regions. Another series was processed using Calbindin immunoreactivity. After staining, histological sections were scanned. Manipulations of the section during this last part of the procedure may also cause uncorrelated non-linear distortions on each section.

We segmented for each section the foreground from the background, using a threshold computed on each slice's histogram. In the course of the staining process, intensity differences occurred among histological sections. To correct this, we normalise all intensity histograms by centering the principal peak (representing the principal organic tissue) of each section.

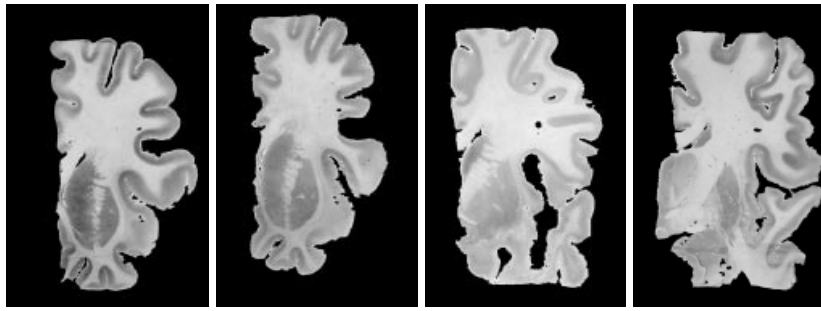

Fig. 1. *Four digitised sections after Nissl staining and background removal.*

3 Fusion of Histology and MR Images

Among the available data (MR T1, MR T2, Nissl and Calbindin), we choose to fuse the T1-weighted MR image with the Nissl histological series because of three reasons: the T1-weighted MR image is less distorted than the MR T2; the Nissl dataset is more similar to the MR T1; Calbindin staining, which needs more intermediate steps than Nissl, produces more distortions.

We choose a twofold approach: 1) construction of a 3D histological block, by 2D realignment of the histological sections; 2) 3D registration of this block with the MR image. Both steps are conducted with the same registration algorithm, which will be presented after a short review of the literature.

3.1 Fusion of Histology and MR Images in the Literature

Image registration is often a key step for biomedical imaging applications. In brain mapping [17], the quality of the atlas construction depends of the quality of the image registration, and in our case the quality of the histology-MR registration. Up to now, only a reduced number of papers have been published on this particular registration problem.

Most of the approaches proposed so far are based on surface matching, i.e. registration of the same anatomical surfaces extracted from both data sets.

In [7], for an Alzheimer's disease study, a 3D elastic warping algorithm is used to deform the contours of the stained sections to the rigid shape imaged in the cryomacrotome. Then, the digital cryovolume is registered to a pre-mortem [^{18}F]fluorodeoxyglucose (FDG) PET using a rigid intensity-based registration algorithm. This way, the authors obtain a 3D correspondence between the stained sections and the FDG-PET. More recently, Jacobs *et al* [4] proposed a methodology for a 2D warping of MRI with rat's brain histological sections. The authors use a surface matching technique for the rigid registration. With the resulting contours, the 2D warping procedure is done using thin-plate splines.

In these first two studies, the authors used the external contours of the brain (cortical surface, ventricles, ...), visible on all the modalities (cryomacro-

tome-stained sections [7], MRI-brain sections [4]) to register the histological sections together and with the 3D image.

In another approach, Schormann *et al* [14] proposed a method based on correlated landmarks. In this article, the authors assume that the histological sections are already aligned. For the histology/MR registration, the user defines interactively a set of reference points in the MR (a sub-volume is defined around these points) and the algorithm finds correspondences using the correlation coefficient criterion. This particular similarity criterion implicitly assumes that there exists a affine relationship between the intensities in sub-volumes to be registered [**?**]. Only small rotations are handled for computational efficiency.

In our application, it was not possible to use contours to register histological sections with the MR. Indeed, the basal ganglia, which are the structures of interest, can hardly be distinguished in the MR. Other structures do not provide enough contours. On the other hand, there is a fairly good functional relationship between the intensities of the MR T1 and the Nissl stained sections. These reasons make us prefer an intensity-based registration method.

We present in section 3.2 a local intensity-based algorithm, which will be used to perform both the reconstruction of the 3D block from histological sections (section 3.3) and the registration of the MR image with the reconstructed block (section 3.4).

3.2 Registration: An Intensity-Based Robust Algorithm

The method is based on a block-matching strategy. First, for each block in the first image, we compute its best corresponding block in the second image, by minimising a local similarity criterion. This criterion can be chosen with respect to the assumed relationship between both images' intensities [**?**]. Processing all blocks yield a set of correspondences, with which a global parametric transformation (e.g. rigid or affine) can then be estimated with a least trimmed squares (LTS) minimisation, which is more robust with respect to outliers than the classical least squares. These two steps are iterated and integrated into a multi-scale scheme.

Within this approach, two choices have to be made: the similarity measure and the class of transformations. We justify our choices for each registration case in sections 3.3 and 3.4.

3.3 Reconstruction of a 3D Block from the Histological Sections

This first registration step consists in reconstructing a 3D histological block from a set of 2D histological sections.

Usually, this step is presented as a trivial preprocessing task (see section 3.1). The main difficulty arises from the fact that two consecutive slices represent two different anatomical sections. Thus, two kinds of shape difference may appear: the first one is related to anatomical changes from section to section, while the second one is due to local distortions induced by the sectioning process. Thanks

to its robustness, our algorithm will exploit only the coherent correspondences, due to local similarities, to find the best transformation, and reject the ones due to large changes or local distortions.

For the 3D alignment of consecutive 2D slices, such as histological sections, we use a 2D version [9] of the block matching algorithm presented in section 3.2. By computing a transformation between each two consecutive sections, we can collect all of them in a single 3D block. Our particular choices for these registrations are the correlation coefficient as similarity measure, and 2D rigid transformations as global parametric transformation.

The correlation coefficient assumes that there exists a affine relationship between the intensities of corresponding blocks of two successive sections. This choice seems to be reasonable for histological data (see Figure 1).

There is a gap of 700 μm between two consecutive histological sections: assuming that anatomy from one slice to the next differs only slightly seems to be reasonable, yielding to the choice of rigid transformations.

Elastic transformations (e.g. affine) may correct some of the observed morphological changes from section to section. However, as we can not distinguish between anatomical changes and local distortions to the histological process, searching such transformations may introduce false deformations and can therefore compromise the next step of the data fusion.

Results In Figure 2, we present the reconstructed 3D block obtained from the histological sections. First, we simply show the stack obtained by putting each digitised original Nissl section on top of the previous one. Then, we see the same block after alignment. Precisely, starting from the slice in the middle of the original stack, we computed rigid transforms from this slice to the next ones, and then, by combining the resulting slice-to-slice transforms, we obtained the reconstructed block. As can be seen, the continuity of both sulci and structures of the basal ganglia has been improved, compared to the original stack. Nevertheless, one can also observe intensity variations between slices, especially on the sagittal and axial views. This is the reason why an intensity normalisation is needed, and it yields the third block, where both misalignments and intensity variations have been corrected. This block is going to be used for the registration of MR and histology images.

3.4 Registration of the Reconstructed Histological Block with the MR Images

Once the 3D histological block has been reconstructed, we have to register it with the 3D MR image, which will be done with a 3D version [**?**] of the block matching algorithm presented in section 3.2.

As the MR T1 acquisition is larger and presents less distortions than the histological 3D image, we will compute a transformation from the block *towards* the MR image, which we consider as a reliable anatomical reference.

As previously explained, the choice of the similarity measure depends on the expected relationship between the intensities of the images to be registered [**?**].

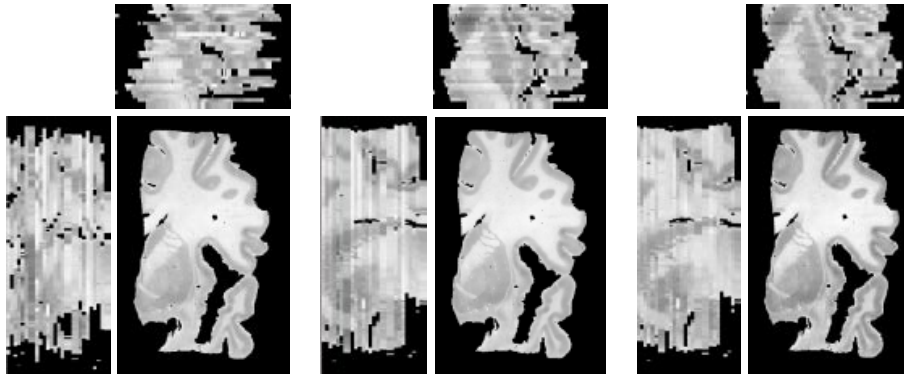

Fig. 2. *Reconstructed 3D block from histological sections; left block: stack of digitised original Nissl sections; middle block: same block after alignment; right block: same block after alignment and intensity normalisation. For each block: bottom left: sagittal view; bottom right: coronal view; top right: axial view.*

In the case of histology and MR images, a reasonable assumption is a functional relationship, and thus we choose the correlation ratio.

Concerning the choice of the transformation to be looking for, we choose affine transformations. Indeed, the histological procedure (section 2.2) has caused global shape changes, that may be captured by such transformations. Unfortunately, the additional uncorrelated in-slice distortions can not be modelized by a 3D transformation, and thus can not be corrected at this point. Nevertheless, we have to point out that the robustness of the estimation procedure allows us to treat them as outliers: thus they will not perturb the estimation of the 3D transformation.

To avoid some local minima during estimation, we perform a *hierarchical global registration*: we first compute a 3D rigid transformation; after convergence, we use it as initialisation for the estimation of the 3D affine registration.

Results We present in Figure 3 results of the affine registration between the reconstructed block obtained in the previous section and the MR T1-weighted image. The registered images have been superimposed and are shown with increasing opacity factors. Each row corresponds to different cuts through the volumes, and shows three slices (sagittal, coronal and axial).

First, the overall impression is that the affine registration provides a fairly good solution. Correspondence of the sulci and the cortex is consistent, see first row (axial and coronal slices), and third row (sagittal slice). Correspondence of the caudate nucleus and putamen is also consistent, see first row (axial slice), and third row (axial and coronal slices). The first (coronal slice) and the second (sagittal slice) rows illustrate that histology / MR registration allows to localise areas that were almost undetectable directly on the MR image.

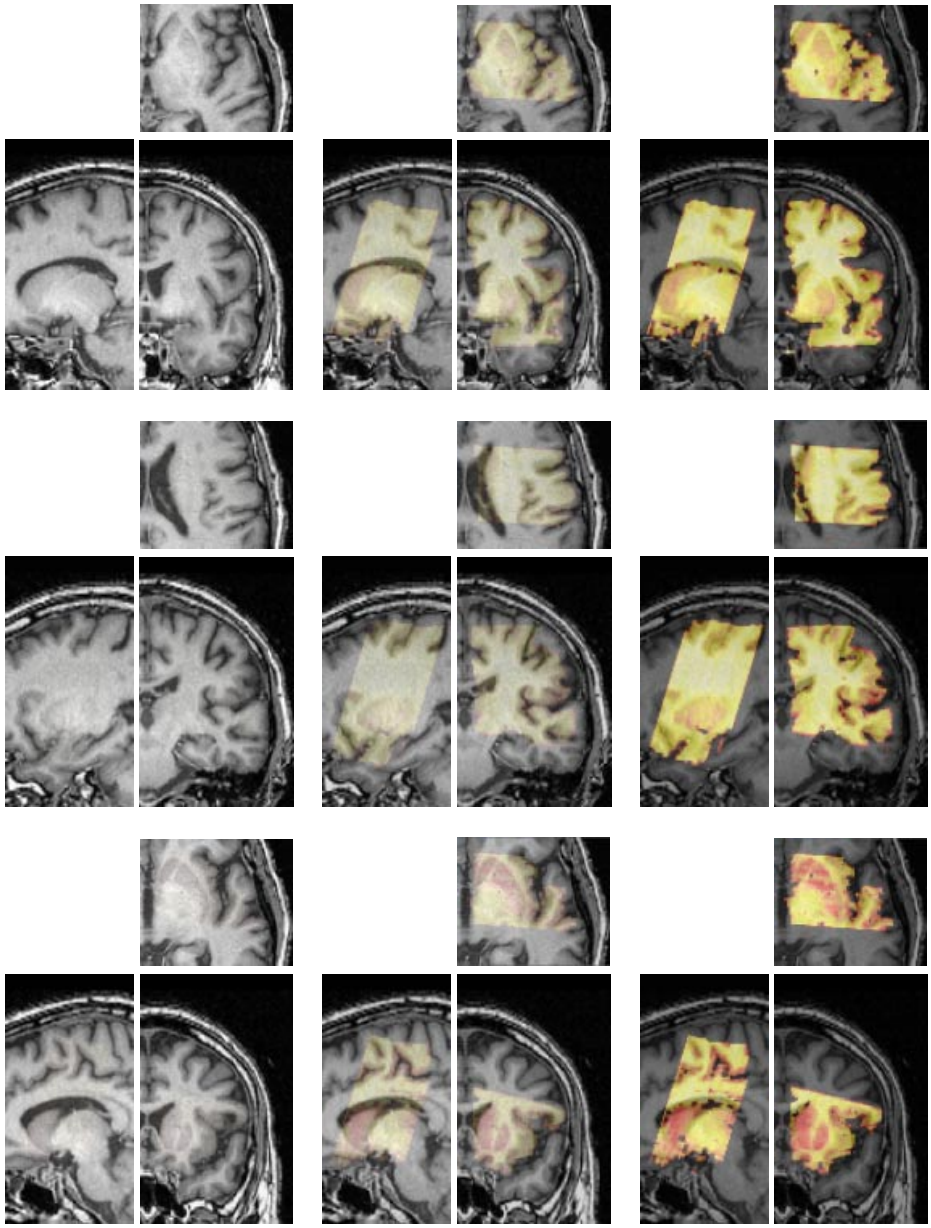

Fig. 3. *Affine registration of reconstructed histological block with MR T1 image. From left to right: MR and histological block are superimposed with increasing opacity factors (left column: MR:1, Histo.: 0; middle: MR:0.5, Histo.: 0.5; right: MR: 0.2, Histo.: 0.8) The three rows show three different cuts through the volumes (see text for details). For each block: bottom left: sagittal view; bottom right: coronal view; top right: axial view.*

Finally, a ventricle collapse occurred during histology, which caused local non-linear distortions. Here again, the affine registration provided a consistent solution, see first (sagittal and coronal slices), second (axial slice) and third (sagittal and coronal slices) rows. Indeed, only the corpus callosum is misregistered (it lies in the ventricle in the MR image). This shows that the slight non-linear distortions were considered as outliers and rejected during the affine transformation computation.

4 Conclusion and Future Work

In this article, we have presented a methodology to fuse 2D histological sections and a 3D MR image. This represents the first step towards the construction of an atlas of the basal ganglia which will be used to determine the target for DBS of parkinsonian patients with higher accuracy. Our method, using an intensity-based robust registration algorithm, allowed us to get, after a first realignment step, an affine correspondence between the histological block and the MR T1-weighted image. The results looked fairly good. Subsequent steps will include the fusion of anatomical contours and the treatment of local non linear distortions by using elastic registration algorithms.

Acknowledgements

This work was partly supported by Medtronic (Research agreement no. 97506). We thank Johan Montagnat for providing the intensity normalisation tool, and Hervé Delingette for the visualisation software.

References

1. A.L. Benabid, P. Pollak, C. Gervason, D. Hoffmann, D.M. Gao, M. Hommel, J. Perret, and J. De Rougemont. Long-term suppression of tremors by chronic stimulation of the ventral intermediate thalamic nucleus. *Lancet*, 337:403–406, 1991.
2. A.L. Benabid, P. Pollak, A. Louveau, S. Henry, and J. De Rougemont. Combined (thalamotomy and stimulation) stereotactic surgery of the vim thalamic nucleus for bilateral parkinson disease. *Appl. Neurophysiol.*, 50:1–6, 1987.
3. D. Dormont, P. Cornu, B. Pidoux, A.M. Bonnet, A. Biondi, C. Oppenheim, D. Hasboun, P. Damier, E. Cuchet, J. Philipon, Y. Agid, and C. Marsault. Chronic thalamic stimulation using 3-dimensional mr stereotaxic imaging. *American Journal of Neuroradiology*, 8:1093–1107, 1997.
4. M.A. Jacobs, J.P. Windham, H. Soltanian-Zadeh, D.J. Peck, and R.A. Knight. Registration and Warping of Magnetic Resonnance Images to Histological Sections. *Med. Phys.*, 26(8):1568–1578, 1999.
5. P. Limousin, P. Pollak, D. Benazzouz, D. Hoffmann, J.F. Le Bas, E. Broussolle, J.E. Perret, and A.L Benabid. Effect of parkinsonian signs and symptoms of bilateral subthalamic nucleus stimulatiom. *Lancet*, 345, 1995.
6. J. B. A. Maintz and M. A. Viergever. A survey of medical image registration. *Medical Image Analysis*, 2(1):1–36, 1998.

7. M.S. Mega, S.S. Chen, P.M. Thompson, R.P. Woods, T.J. Karaca, A. Tiwari, H.V. Vinters, G.W. Small, and A.W. Toga. Mapping Histology to Metabolism: Coregistration of Stained Whole-Brain Sections to Premortem PET in Alzheimer's Disease. *Neuroimage*, 5:147–153, 1997.
8. S. Ourselin, A. Roche, S. Prima, and N. Ayache. Block Matching: A General Gramework to Improve Robustness of Rigid Registration of Medical Images. In A.M. DiGioia and S. Delp, editors, *Third International Conference on Medical Robotics, Imaging And Computer Assisted Surgery (MICCAI 2000)*, pages 557–566, Pittsburgh, Pennsylvania USA, October 11-14 2000.
9. S. Ourselin, A. Roche, G. Subsol, X. Pennec, and N. Ayache. Reconstructing a 3D Structure from Serial Histological Sections. *Image and Vision Computing*, 19(1-2):25–31, January 2001.
10. A. Roche, G. Malandain, N. Ayache, and S. Prima. Towards a Better Comprehension of Similarity Measures used in Medical Image Registration. In *Proc. MICCAI'99*, volume 1679 of *LNCS*, pages 555–566, Cambridge (UK), October 1999.
11. A. Roche, G. Malandain, X. Pennec, and N. Ayache. The Correlation Ratio as a New Similarity Measure for Multimodal Image Registration. In *First International Conference on Medical Image Computing and Computer-Assisted Intervention*, volume 1496 of *Lecture Notes in Computer Science*, pages 1115–1124, Cambridge (USA), October 1998. Springer.
12. Peter J. Rousseuw and Annick M. Leroy. *Robust Regression and Outlier Detection.* Wiley Series in Probability and Mathematical Statistics, first edition, 1987.
13. G. Schaltenbrand and W. Wharen. *Atlas for Stereotaxy of the Human Brain.* Stuttgart: Georg Thieme Verlag, 1977.
14. T. Schormann, M. Von Matthey, A. Dabringhaus, and K. Zilles. Alignment of 3-D Brain Data Sets Originating From MR and Histology. *Bioimaging*, 1:119–128, 1993.
15. J. Talairach and P. Tournoux. *Co-planar Stereotaxic Atlas of the Human Brain.* New York: Thieme Medical Publishers, Inc., 1988.
16. P.M. Thompson and A. Toga. A Surface-Based Technique for Warping Three Dimensional Images of the Brain. *IEEE Transaction on Medical Imaging*, 15:1–16, 1993.
17. A.W. Toga and P.M. Thompson. The Role of Image Registration in Brain Mapping. *Image and Vision Computing*, 19(1-2):3–24, January 2001.
18. M. Yoshida. Creation of a Three-Dimensional Atlas by Interpolation from Schaltenbrand-Bailey's Atlas. *Appl. Neurophysiol*, 50:45–48, 1987.